Supporting Information Appendix

Resuscitation of *Pseudomonas aeruginosa* from dormancy requires hibernation promoting factor (PA4463) for ribosome preservation

Tatsuya Akiyama, Kerry S. Williamson, Robert Schaefer,
Shawna Pratt, Connie B. Chang, and Michael J. Franklin

Table of Contents

SI Text S1. Full materials and methods.

SI Figure S1. Recovery following incubation under nutrient deprived conditions.

SI Figure S2. Colony morphology following incubation under nutrient deprived conditions.

SI Figure S3. Recovery of a stringent response mutant following incubation under nutrient deprived conditions.

SI Figure S4. Bioanalyzer RNA profiles from nutrient deprived cultures.

SI Figure S5. Bioanalyzer RNA profiles from additional strains following nutrient deprivation.

SI Figure S6. Quantification of RNA loss and RNA fragment buildup following incubation under nutrient deprived conditions.

SI Figure S7. Histograms showing 16S fluorescence in situ hybridization (FISH) of cells following incubation under nutrient deprived conditions.

SI Figure S8. Box and Whisker plots of 16S rRNA abundance of starved cells determined by FISH.

SI Figure S9. Quantification of cells that remain as single cells and those capable of regrowth inside microfluidic drops following starvation.

SI Figure S10. Example of cell resuscitation within oil drops in PBS starvation medium.

SI Figure S11. Growth rates within individual microfluidic drops containing TSB.

SI Table S1. P-values used to determine a significant difference between PAO1 and Δ*hpf* FISH intensities under nutrient deprived conditions.

SI Table S2. P-values used to determine no significant difference between PAO1 and PAO1 Δ*hpf* + *hpf* FISH intensities under nutrient deprived conditions.

SI Movie S1. Growth of *P. aeruginosa* PAO1 (pMF230) in microfluidic drops containing TSB medium, following four days of incubation under nutrient deprived conditions.

SI Movie S2. Growth of *P. aeruginosa* PAO1 Δ*hpf* (pMF230) in microfluidic drops containing TSB medium, following four days of incubation under nutrient deprived conditions.

SI, Materials and Methods

Bacterial strains and growth conditions

Studies were performed on *Pseudomonas aeruginosa* strain PAO1 and its Δ*rmf* and Δ*hpf* deletion mutant derivatives, which were described previously and generated using the PCR primers described previously (1). The Δ*hpf*/Δ*rmf* double mutant was also constructed using the allelic exchange approach with the same PCR primers (1), with *rmf* deleted from the Δ*hpf* mutant. The stringent response mutant strain, containing deletions of *relA* and *spoT* (2) was graciously provided by Dr. Pradeep Singh. The Δ*hpf* and Δ*rmf* mutant strains were complemented with plasmids constructed as follows: fragments of *hpf* and *rmf* were amplified using primers: Rmf XbaI5' (5'-AGTCTAGAAGTGAGGGCAACACCCTATG), Rmf HindIII 3' (5'-TTAAGCTTGCGC-CCGCCGCCCGGATG), HPF XbaI 5' (5'-CATCTAGACACGGGCAACAAGGAGAACGC), HPF HindIII 3' (5'-TCAAGCTTTGCTCAAGTCGGATCATAG). The PCR products were ligated into the plasmid vector pMF54, which contained an IPTG-inducible promoter. The resulting plasmids were labeled pMF462 for *rmf*, and pMF466 for *hpf*. In certain experiments, the Δ*relA*/Δ*spoT* strain was also complemented with the *hpf*-containing plasmid, pMF466. The plasmid pMF230, described in (3) was introduced into strains to provide constitutive expression of the green fluorescent protein (GFP) for confocal scanning laser microscopy (CSLM) analyses. Strains were cultured on trypticase soy agar (TSA) using gentamicin (100 μg x ml^{-1}),

carbenicillin (150 µg x ml^{-1}), and 1.0 mM isopropyl ß-D-1-thiogalactopyranoside (IPTG) when necessary.

Nutrient starvation studies

Frozen stock strains were cultured overnight in TSB. For strains containing plasmids, the TSB was supplemented with 150 µg x ml^{-1} carbenicillin and 1.0 mM IPTG to induce expression of *hpf* or *rmf*. An aliquot (120 µl) of the overnight culture was used to inoculate 4 ml of TSB. The cultures were incubated at 37ºC with aeration for 7 h, until the optical density (OD_{600}) was a minimum of 7.0 on a CE2041 Spectrophotometer (Cecil Instruments). An aliquot of the culture was centrifuged and the pellet was washed twice in phosphate buffered saline solution (PBS), pH 7.0. The resulting cell pellets were resuspended in 1 ml PBS and used to inoculate 25 ml of pre-warmed PBS in 125 ml baffled flasks to obtain an initial cell concentration of 1.5×10^8 CFU x ml^{-1}. Cultures were continuously incubated at 37ºC with shaking at 200 rpm and were sampled after 30 min and then daily for use in cell viability, rRNA abundance, fluorescence *in situ* hybridization, and microfluidic drop assays.

Determination of cell viability

The drop plate method was used to quantify colony forming units. Briefly, cells were serially diluted in 0.85% NaCl solution and 100 µl volumes were plated on TSA (4). Colonies were counted after 18 h of incubation at 37ºC, and again at

42 h. Six biological replicates were performed for the wild type and single knockout strains at each time point. A minimum of three biological replicates were performed for the additional seven mutant strains. The mean and standard error of the mean (SEM) were calculated for the recovering colonies and plotted using GraphPad Prism 7.01. GraphPad Prism was also used to perform t-tests and one and two-way ANOVAs at alpha < 0.05.

RNA extraction and determination of relative 23S and 16S rRNA abundances

At each time point, cells were collected by centrifugation at 7,800 x g for 1 min at 4ºC. After removal of the supernatant, cell pellets were stored at -80ºC until RNA extraction. Total RNA was extracted similar to that described previously (5). Briefly, cell pellets were resuspended in a mixture of 50 µl lysis buffer and 50 µl of sodium dodecyl sulfate (SDS). After the addition of 100 µl phenol, the reaction mixture was incubated at 65ºC for 5 min with vortexing. The mixture was centrifuged to allow for phase separation, and 100 µl of phenol:chloroform:isoamyl alcohol solution was added to the aqueous phase. Following a second phase separation step, the Clean and Concentrator-5 kit (Zymo Research) was used on the aqueous phase as per the manufacturer's instructions. RNA was then measured on the NanoDrop1000 (Thermo Fisher Scientific), diluted to approximately 50 ng x μl^{-1}, and visualized on the Bioanalyzer 2100 (Agilent Technologies) with the Prokaryotic Total RNA 6000 Nanoassay (Agilent Technologies). The ratio of 23S rRNA to 16S rRNA was

plotted using GraphPad Prism 7.01 as the mean and standard error of the mean for three to four biological replicates. GraphPad Prism was also used to perform t-tests and one and two-way ANOVAs at alpha < 0.05. For fragment analysis, the time corrected area from the peak at 100 nucleotides (comprised of RNA fragments and 5S rRNA) was divided by the total time corrected area of the total RNA detected for each sample. The mean and SEM for 3 to 4 biological replicates were plotted in GraphPad Prism.

Quantification of total rRNA, and quantification of 16S and 23S rRNAs by RT-qPCR.

During starvation, 100 μl cell suspensions were frozen daily at -80C and stored until RNA extraction was performed as above, but with the following modifications: 20 μl of 10x lysis buffer/SDS was added to the cell suspension, the incubation time was extended to 8 min, and a heavy phase lock gel (5 Prime) was used to ensure complete RNA recovery. RNA yield was measured in triplicate for each sample on the NanoDrop1000 (Thermo Fisher Scientific), using a minimum of three biological replicates. The mean ng RNA recovered per μl of starvation culture and standard error of the mean were plotted using GraphPad Prism 7.01, and a t-test was performed at alpha < 0.05. One-step reverse transcription-quantitative PCR (RT-qPCR) was performed with the Rotor-Gene SYBR green RT-PCR kit (Qiagen) as described previously (46) with 16S_F primer (TACCTGGCCTTG ACATGCTG), 16S_R primer

(CCCAACATCTCACGACACGA), 23S_F primer (TGTGGATCGGAGTGAAAGGC) and 23S_R primer (AGCCGAAACAGTGCTCTACC), using 2 μl of a 1:1000 dilution of turbo-DNase (ThermoFisher Scientific) treated recovered RNA as the template in each reaction. Reactions were performed in triplicate on three biological replicates for each strain at 0 and 4 days of starvation. RT-qPCR primer efficiencies, calculated from the slope of standard curves using Rotor-Gene software, were similar for 16S (0.96) and 23S (0.98) primers. Negative controls lacking reverse transcriptase were performed with each biological sample, and revealed that samples were free from DNA contamination. The Relative Expression Software Tool V2.0.13 (REST) (6) was used to calculate mean fold change of 16S and 23S RNA recovered in the Δ*hpf* strain compared to wild type PAO1 and to interpret significance at $\alpha \leq 0.05$. Mean relative expression and standard error of the mean were plotted in GraphPad Prism.

Fluorescence in situ hybridization (FISH) for quantification of ribosomal RNAs

Fluorescence *in situ* hybridization (FISH) was used to quantify the relative amounts of 16S RNA from individual cells following starvation conditions. An aliquot, 1 to 2 ml, of nutrient-deprived cells was centrifuged, washed with PBS, then resuspended in 100 µl of ice-cold PBS. Resuspended cells were fixed with 300 µl of 4% paraformaldehyde, and incubated at 4ºC for 3 h. Fixed cells were washed with ice-cold PBS twice, resuspended in 50-100 µl of ice-cold 50% ethanol:PBS solution, and stored at -20ºC, prior to visualization.

FISH was performed as described by Brileya et al. (7). Fixed cells were dried on 10 well poly-L-lysine coated teflon-printed microscope slides (Tekdon, Inc.), and dehydrated by incubating slides in increasing concentrations of ethanol (50, 80, and 100%) for 3 min each. Fixed cells were incubated at 46ºC for 2 h in the dark in hybridization buffer (0.9 M NaCl, 20 mM Tris-Hcl, pH 8.0, 0.01% SDS) which contained probes targeting 16S rRNAs, using oligonucleotide sequences described by Hogardt *et al.* (8). The 16S rRNA probe (PseaerA) and 23S probe (PseaerB) were labeled with Cy3 and ATTO™647N, respectively (Integrated DNA Technologies, Inc.). After incubation, slides were washed with 0.9 M NaCl, 20 mM Tris-HCl, pH 8.0 at 48ºC for 10 min. Slides were dipped in ice-cold water and dried with compressed air. Citifluor Antifadent mounting medium, AF-1 (Electron Microscopy Sciences), and a coverslip were placed onto the slides and cells were imaged using an epifluorescent microscope. Filters used are as follows: FITC for GFP, 480/30 excitation, 505LP mirror, 535/40 emission; TRITC for 16S-Cy3, 540/25 excitation, 565LP mirror, 605/55 emission; Cy5 for 23S-ATTO™647N, 620/60 excitation, 660LP mirror, 700/75 emission. Three biological replicates were used for the FISH experiments for each strain and each time point. Five to seven fields were imaged for each biological replicate and time point. The images were analyzed using ImageJ (http://imagej.nih.gov/ij/). Only 16S rRNA data are reported in this study. For quantification, background was subtracted using a rolling ball background subtraction algorithm in ImageJ with the rolling ball radius set for 200 pixels. The edge of each cell was

determined using the Canny Edge Detector plugin in ImageJ. The edge of each cell was selected as a region of interest (ROI) and overlaid on images for Cy3 and FITC. The overlaid ROI was adjusted using the ROI Manager Move Selection macro in ImageJ and mean gray value per pixel within the ROI was measured and used to indicate the abundance of 16S rRNA, and GFP. To reduce the fluctuations in fluorescence intensity caused by technical errors, such as differences in the hybridization efficiency and photo-bleaching among experiments, exponential phase *P. aeruginosa* PAO1 (pMF230) was used as an internal spike-in control, and mean gray values of samples were normalized to the spike-in control for each picture as follows: the total average mean gray value per pixel of spike-in control cells was determined for every slide. The ratio of the average mean gray value for the spike-in cells per picture to the total average mean gray value for spike-in cells was used to normalize the mean gray value per pixel for cells of interest for each picture. Welch's t-tests (unequal variance t-test) and Kruskal-Wallis tests (one-way ANOVA on ranks) at alpha = 0.05 were performed on the average normalized background subtracted intensities of each biological replicate in Graphpad Prism.

Drop encapsulation and monitoring growth of single bacterial cells

P. aeruginosa PAO1 and the Δ*hpf* mutant constitutively expressing the GFP from pMF230 were incubated under starvation conditions as described above. The cultures, 100 µl, were mixed with 900 µl of TSB. 1 ml of each cell

culture and 2 ml of fluorocarbon oil (3M HFE 7500) with 1.2 to 1.5% w/w of a biocompatible PFPE-PEG fluorinated surfactant (9) were injected to a 15 µm drop making chip with flow focusing features. Flow rates for the two aqueous phases, cell resuspension and HFE, were 100 µl x h^{-1} and 375 µl x h^{-1}, respectively. Encapsulated cells were collected in syringes and incubated at 37ºC for 24 and 48 h. The emulsions were gently agitated using a Hula Mixer set to 30º at 1 rpm. Drops were re-injected into a modified “Dropspots” immobilization device (10), which allows for a monolayer of drops to be immobilized in an array of round chambers, and imaged using an inverted confocal microscope (Leica TSC SP2). Three biological replicates were prepared and three to five images at three different magnifications (a total of nine to eleven images) per biological replicate were collected. Images were taken using a 473 nm excitation wavelength (argon laser), a PMT detection range of 500-550 nm, a 20x long working distance objective, and a z resolution of 1.5 µm. Magnifications were adjusted using Leica’s microscopy software such that magnification 1 captured 250-400 drops, magnification 2 captured 125-200 drops, and magnification 3 captured 15-25 drops. Images were analyzed using MetaMorph and ImageJ softwares, where drops containing single cells were differentiated from drops containing higher amounts by creating maximum projection reconstructions. Additionally, single cells were differentiated from artifacts by scanning through each slice examining for cell motility. To test for statistical significance, Welch’s t-tests (unequal variance t-test), an ANOVA, and Kruskal-

Wallis tests (one way ANOVA on ranks) were performed in Graphpad Prism at alpha < 0.05.

For real-time imaging of bacterial growth within drops, a Dropspot device was prepared by bonding the molded PDMS slab to a coverslip, and then bonding this device to a petridish with a coverslip viewing window. The entire assembly was soaked under a layer of HFE7500 and water for a minimum of 12 h at 70°C, and allowed to cool for 30 min. Fifteen μm drops containing TSB, inoculated with single cells, were placed into the 50 μm well diameter PDMS Dropspot device. The Dropspot device was incubated in a microscope stage environmental chamber at 37°C with 75% relative humidity. Drops were imaged every 10 min at 10x magnification for 24 h. Bacterial growth rate within drops was calculated using image analysis software ImageJ with the Fiji image processing package (11). The TrackMate plugin (12) was used to identify and track the fluorescent intensity over time of drops with cell growth frame-by-frame, allowing the automatic identification of active drops with minor user input for filtering incorrectly tracked drops. The text file output from TrackMate was then loaded into a custom MATLAB script for the calculation of a maximum growth rate (μmax) for each drop by taking the natural log of the linear region of the growth curve. We assumed that the fluorescence intensity of the drops was linearly correlated with the concentration of cells within the drops over the range of the PMT output on the confocal microscope (13).

1. Williamson KS*, et al.* (2012) Heterogeneity in *Pseudomonas aeruginosa* biofilms includes expression of ribosome hibernation factors in the antibiotic-tolerant subpopulation and hypoxia-induced stress response in the metabolically active population. *J Bacteriol* 194(8):2062-2073.
2. Nguyen D*, et al.* (2012) Active starvation responses mediate antibiotic tolerance in biofilms and nutrient-limited bacteria. *Science* 334(6058):982-986.
3. Nivens DE, Ohman DE, Williams J, & Franklin MJ (2001) Role of alginate and its O acetylation in formation of *Pseudomonas aeruginosa* microcolonies and biofilms. *J Bacteriol* 183(3):1047-1057.
4. Herigstad B, Hamilton M, & Heersink J (2001) How to optimize the drop plate method for enumerating bacteria. *J Microbiol Methods* 44(2):121-129.
5. Guragain M*, et al.* (2016) The *Pseudomonas aeruginosa* PAO1 two-component regulator CarSR Regulates calcium homeostasis and calcium-induced virulence factor production through its regulatory targets CarO and CarP. *J Bacteriol* 198(6):951-963.
6. Pfaffl MW, Horgan GW, & Dempfle L (2002) Relative expression software tool (REST) for group-wise comparison and statistical analysis of relative expression results in real-time PCR. *Nucleic Acids Res* 30(9):e36.
7. Brileya KA, Camilleri LB, & Fields MW (2014) 3D-fluorescence in situ hybridization of intact, anaerobic biofilm. *Methods Mol Biol* 1151:189-197.
8. Hogardt M*, et al.* (2000) Specific and rapid detection by fluorescent in situ hybridization of bacteria in clinical samples obtained from cystic fibrosis patients. *J Clin Microbiol* 38(2):818-825.
9. Holtze C*, et al.* (2008) Biocompatible surfactants for water-in-fluorocarbon emulsions. *Lab Chip* 8(10):1632-1639.
10. Schmitz CH, Rowat AC, Koster S, & Weitz DA (2009) Dropspots: a picoliter array in a microfluidic device. *Lab Chip* 9(1):44-49.
11. Schindelin J*, et al.* (2012) Fiji: an open-source platform for biological-image analysis. *Nat Methods* 9(7):676-682.
12. Tinevez JY*, et al.* (2016) TrackMate: An open and extensible platform for single-particle tracking. *Methods*.
13. Baraban L*, et al.* (2011) Millifluidic droplet analyser for microbiology. *Lab Chip* 11(23):4057-4062.

Supplementary Tables

Table S1. Resulting p-values from Welch's t-test between PAO1 and Δ *hpf* FISH intensities, showing a significant difference between the strains over time, after Day 0, under starvation conditions.

	16S
Day1	0.009
Day 2	0.016
Day 3	0.016
Day 4	< 0.001

Table S2. Resulting p-values from Welch's t-test between PAO1 and the complemented strain (Δ *hpf* + *hpf*) FISH intensities, showing no significant difference between the strains over time under starvation conditions.

	16S
Day 0	0.755
Day1	0.893
Day 2	0.602
Day 3	0.395
Day 4	0.130

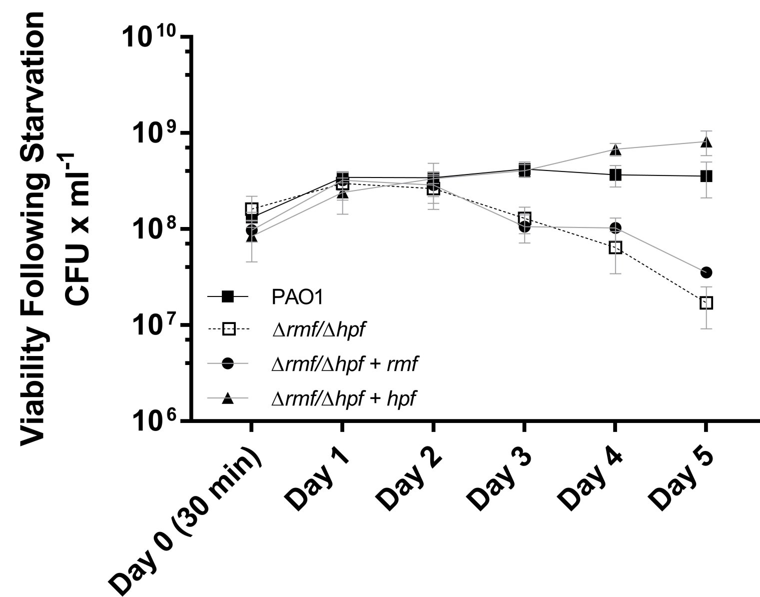

Figure S1. Recovery of *P. aeruginosa* following extended incubation under nutrient deprived conditions. Colony Forming Units (CFU) on TSA agar following incubation in aerated phosphate buffered saline (PBS). Closed Squares – *P. aeruginosa* PAO1; Open Squares – PAO1 Δ*hpf*/Δ*rmf* double mutant; Circles - PAO1 Δ*hpf*/Δ*rmf* complemented with *rmf* (Δ*hpf*/Δ*rmf* + *rmf*); Triangles – PAO1 Δ*hpf*/Δ*rmf* complemented with *hpf* (Δ*hpf*/Δ*rmf* + *hpf*). The mean and standard error of the mean of a minimum of three biological replicates are shown.

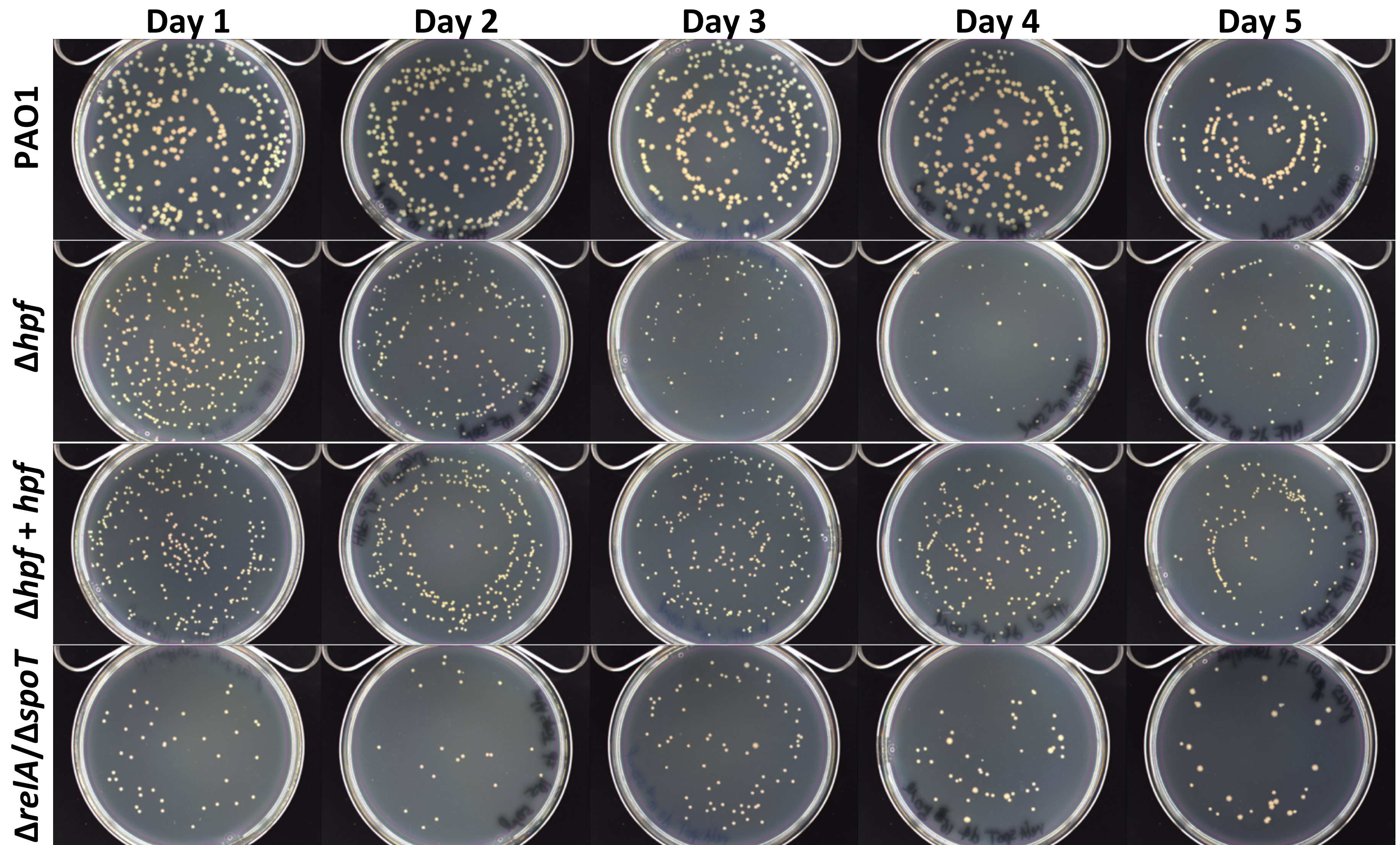

Figure S2. Colony morphology of *P. aeruginosa* PAO1 and its mutant derivatives following incubation in PBS with shaking at 37ºC, then plating on TSA medium. *P. aeruginosa* PAO1 wild-type cells had homogenous colony morphology throughout starvation conditions, whereas the Δ*hpf* mutant had non-uniform colony morphology with extended incubation in PBS. Uniform colony morphologies were restored by complementing *hpf in trans* (Δ*hpf* + *hpf*), although colonies were smaller than the wild-type strain. The Δ*relA*/Δ*spoT* strain had heterogeneous colony morphology, but with no colonies requiring extended incubation to become visible.

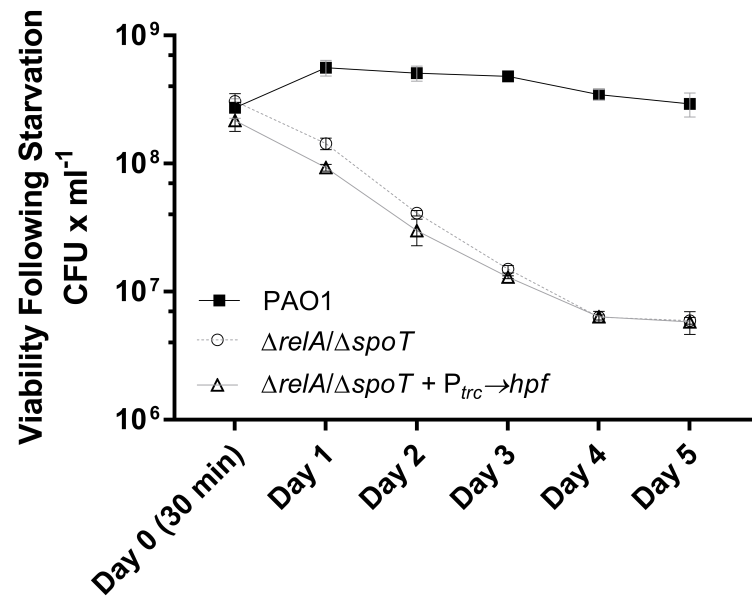

Figure S3. Recovery of *P. aeruginosa* stringent response mutant containing a plasmid copy of *hpf* following starvation. Closed Squares – *P. aeruginosa* PAO1; Circles – PAO1 Δ*relA*/Δ*spoT* double mutant; Triangles – PAO1 Δ*relA*/Δ*spoT* complemented with P_{trc}-> *hpf* (Δ*relA*/Δ*spoT* + *hpf*). The mean and standard error of the mean for three biological replicates are plotted.

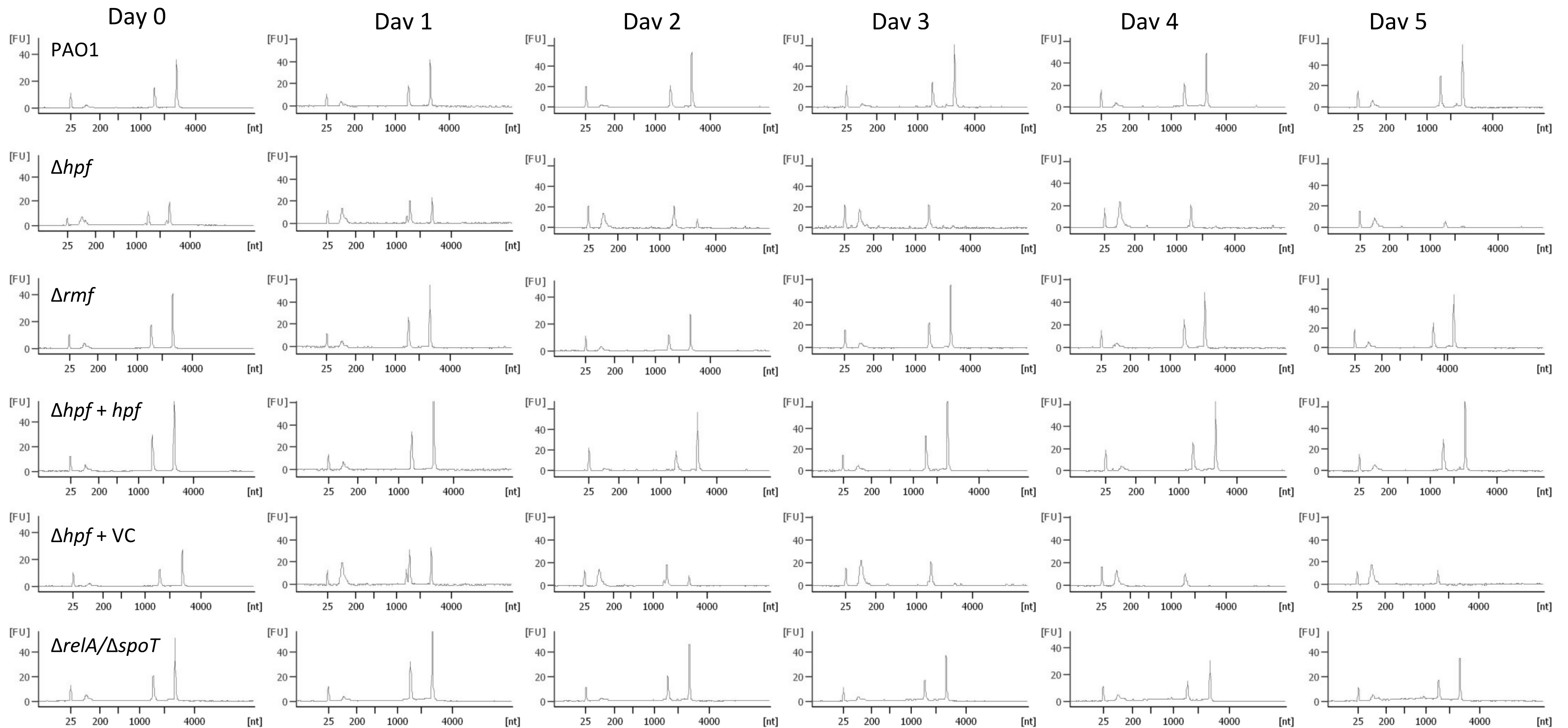

Figure S4. Agilent Bioanalyzer profiles showing 23S and 16S rRNA levels from nutrient deprived *P. aeruginosa* cultures. *P. aeruginosa* PAO1 and PAO1 Δ*rmf* maintained rRNA ratios similar to non-starved cultures throughout incubation. The PAO1 Δ*hpf* strain selectively lost most 23S rRNA by day 3 of starvation. The 23S/16S rRNA levels were restored in the Δ*hpf* mutant when *hpf* was complemented *in trans* (Δ*hpf* + *hpf*), but not with the vector control (Δ*hpf* + VC). The Δ*relA*/Δ*spoT* mutant had 23S/16S ratios similar to the wild-type strain. Representative images shown were selected from a minimum of three biological replicates per strain and time point.

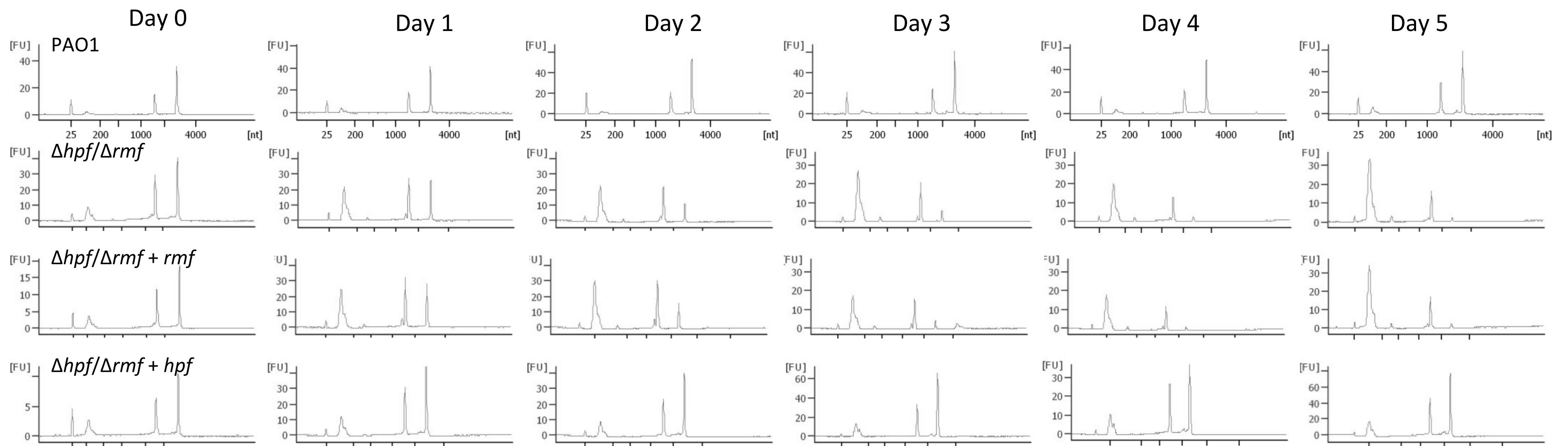

Figure S5. RNA profiles from nutrient deprived *P. aeruginosa* PAO1 Δ*hpf*/Δ*rmf* double mutants, and double mutants complemented with either *rmf* or *hpf* (Δ*hpf*/Δ*rmf* + *rmf*, Δ*hpf*/Δ*rmf* + *hpf*). The double mutant had preferential loss of 23S rRNA, and the 23S/16S rRNA ratio was restored to the wild-type level with *hpf*, but not with *rmf*.

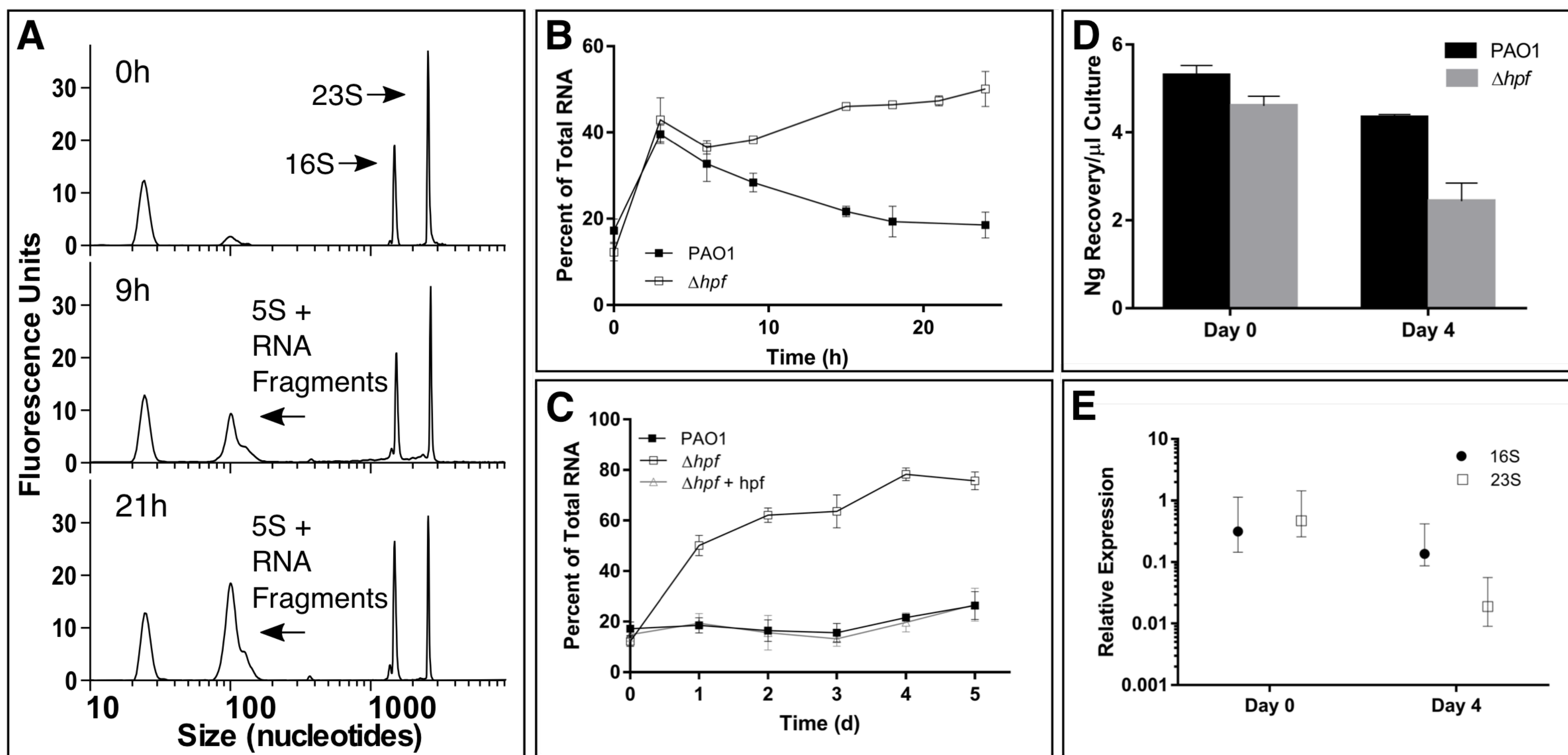

Figure S6. (A) RNA profiles from nutrient deprived *P. aeruginosa* PAO1 Δ*hpf*, within the first day of starvation, showing an increase in the amount of small, degraded RNA fragments as the 23S rRNA decreases. (B) Percentage of the total cellular RNA associated with small RNA fragments for *P. aeruginosa* PAO1 (filled squares) and the Δ*hpf* mutant strain (open squares) over the first 24 h of starvation. Percentage of total RNA was calculated as described in the materials and methods. (C) Percentage of total cellular RNA associated with small RNA fragments over 5 days of starvation for PAO1 (filled squares), the Δ*hpf* mutant (open squares), and the Δ*hpf* mutant complemented with *hpf* (open triangles), showing accumulation of small RNA fragments in the Δ*hpf* mutant strain. (D) Total RNA recovered from PAO1 and the Δ*hpf* strains following zero and four days of starvation. (E) Relative abundances of 16S and 23S rRNA for the Δ*hpf* strain compared to the wild-type control after zero and four days of starvation, determined by RT-qPCR, as described in the methods. Graphs B-E show the mean and standard error of the mean for at least three biological replicates.

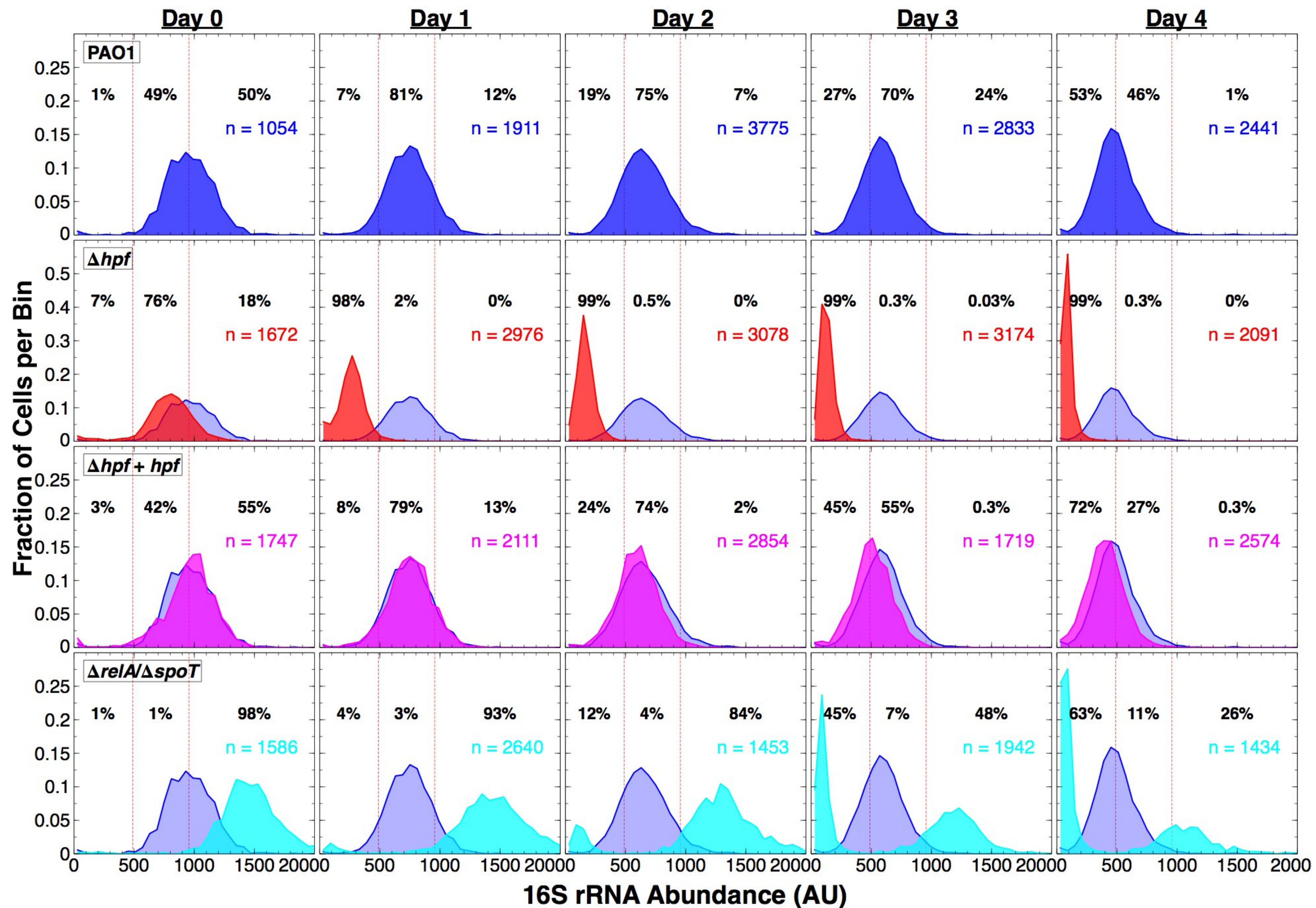

Figure S7. Fluorescent in situ hybridization (FISH) analysis of PAO1, Δ*hpf*, Δ*hpf* + *hpf*, and *relA/SpoT* strains, using the 16S-Cy3 probe. Fluorescence intensity was quantified as described in the methods and individual cell fluorescence intensity was binned. The red dotted vertical lines represent the average FISH fluorescence intensity for the wild-type strain prior to starvation and after four days of starvation. Data for the wild type strain are shown for comparison on each plot in blue. Data shown are from three independent biological replicates per strain at each time point, with the total number of cells quantified indicated. Data points with 16S rRNA abundance higher than 2000 are not shown. *P. aeruginosa* PAO1 shows a normal distribution of fluorescence intensities that gradually decreases with time of starvation. The Δ*hpf* mutant shows a rapid loss of 16S rRNA for most cells. The loss of rRNA in the Δ*hpf* mutant is restored by providing *hpf in trans* (Δ*hpf* + *hpf*). The Δ*relA*/ Δ*spoT* mutant shows a bimodal distribution of 16S FISH-fluorescence intensities with a population of cells having greater 16S rRNA amounts than the wild-type strain, and a population of cells with low 16S rRNA levels. Box-Whisker plots showing the average and range of these data are shown in Fig S8.

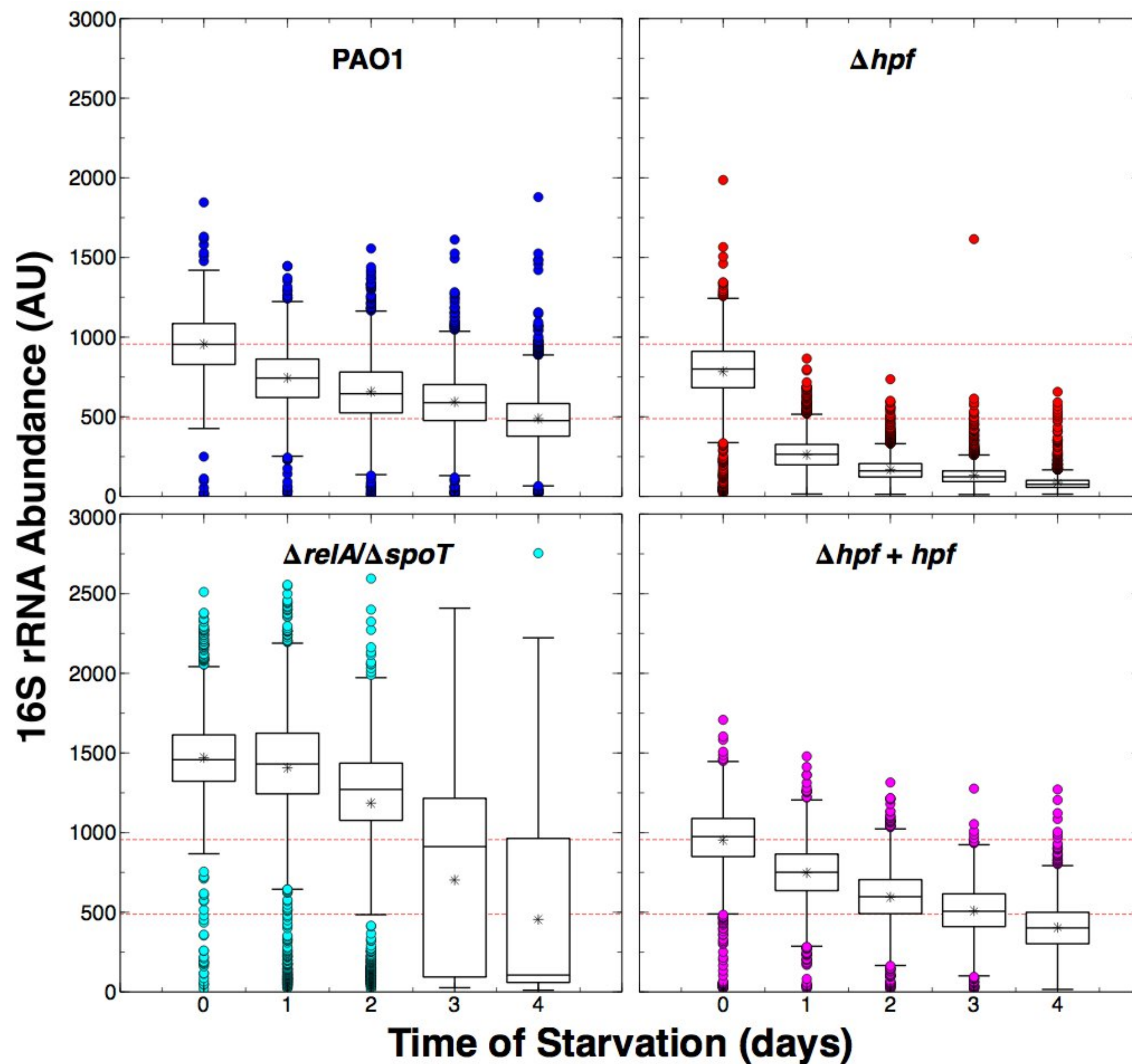

Figure S8. Box and Whisker plot representation of 16S rRNA abundance of starved cells determined by image analysis of FISH data. Shown are wild-type *P. aeruginosa* PAO1 (Blue); PAO1 Δ*hpf* (Red); PAO1 Δ*hpf* complemented with *hpf* (Δ*hpf* + *hpf*) (Magenta); PAO1 Δ*relA*/Δ*spoT* (Cyan). The two red dotted horizontal lines in each plot represent the mean FISH intensity for *P. aeruginosa* PAO1 prior to starvation and after four days of starvation. Boxes correspond to the 25th and 75th percentile of the FISH-fluorescence intensities for individual cells, and the whiskers spread 1.5 internal quartile range (IQR) from the 25th and 75th percentiles. The data plotted as circles outside of 1.5 IQR are considered outliers. The data represent results from three independent biological replicates.

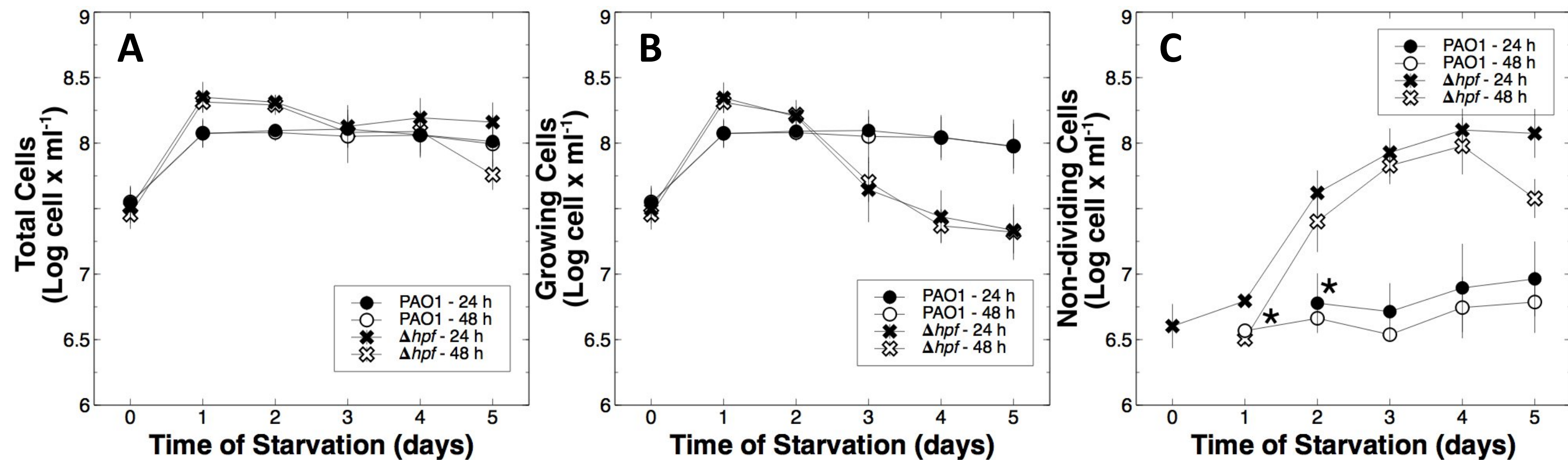

Figure S9. Cells capable of regrowth inside of microfluidic drops and cells that remain as single cells within drops. (A) Total number of cells encapsulated into drops calculated per milliliter of starvation culture, including both cells capable of regrowth and cells that remained as single cells within drops. The total cell numbers were quantified after 24 h and after 48 h incubation in drops. (B) Number of cells that resuscitated within drops. Filled and Open Circles – *P. aeruginosa* PAO1 cells that grew within drops at 24 h and at 48 h; Filled and Open Crosses – PAO1 Δ*hpf* cells that grew within drops at 24 h and 48 h. (C) Number of cells that remained as single cells within drops. Filled and Open Circles – *P. aeruginosa* PAO1 cells that did not grow within drops at 24 h and at 48 h, respectively; Filled and Open Crosses – PAO1 Δ*hpf* cells that did not grow within drops at 24 h and 48 h. Data from three biological replicates are plotted, error bars show the standard error of the mean.

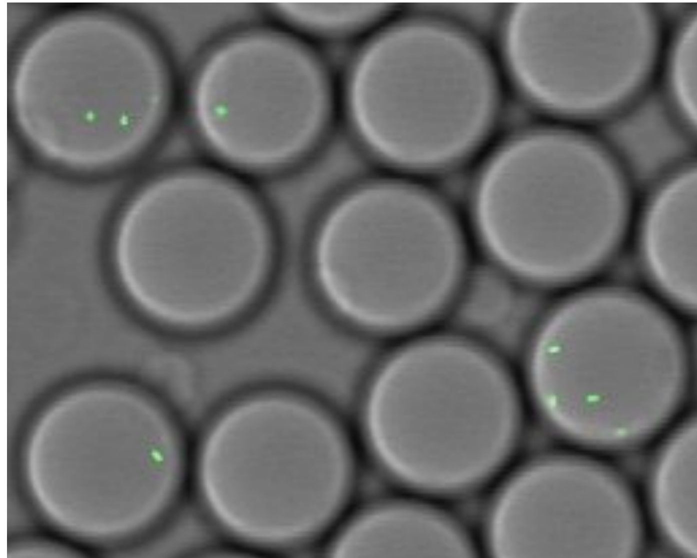

Figure S10. Determination of cell growth in PBS starvation medium. *P. aeruginosa* PAO1 cells were incubated to stationary phase, washed in PBS, then encapsulated in 15 µm diameter oil drops containing PBS. Drops were incubated for 24 h at 37ºC, then examined by confocal scanning laser microscopy. *P. aeruginosa* PAO1 showing multiple cells within drops, indicating that some cells divided at least once during one day of incubation in PBS.

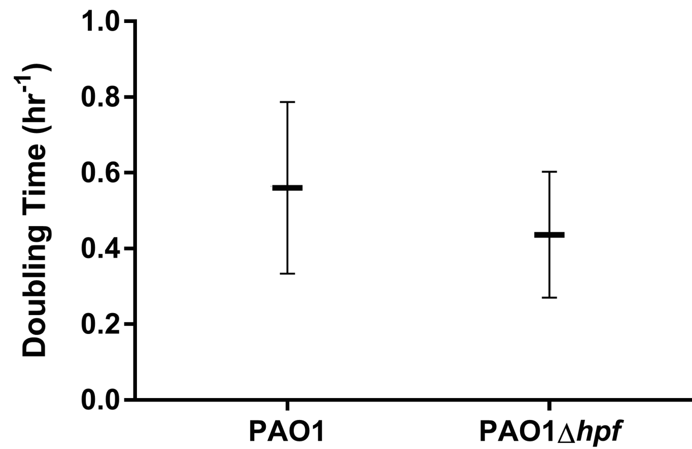

Figure S11. Growth rate of *P. aeruginosa* PAO1 and *P. aeruginosa* PAO1 Δ*hpf* within individual microfluidic drops containing TSB, incubated at 37°C, calculated as described in the materials and methods. Results show the average and standard deviation from three independent biological replicates for each strain. Mean and standard deviation were calculated for 848 drops that had cell growth for PAO1, and 75 drops that had cell growth for PAO1 Δ*hpf*.